Complex Spike Patterns in Olfactory Bulb Neuronal Networks

Alister U. Nicol, Anne Segonds-Pichon, and Magnus S. Magnusson

Abstract

Using T-pattern analysis, a procedure developed for detecting a particular kind of nonrandomly recurring hierarchical and multi-ordinal real-time sequential patterns (T-patterns), we have inquired whether such patterns of action potentials (spikes) can be extracted from extracellular activity sampled simultaneously from many neurons across the mitral cell layer of the olfactory bulb (OB). Spikes were sampled from urethane-anesthetized rats over a 6 h recording session, or a period lasting as long as permitted by the physiological condition of the animal. Breathing was recorded as markers of peak inhalation and exhalation. Complex t-patterns of up to ~20 elements were identified with functional connections often spanning the full extent of the array. A considerable proportion of these sequences were related to breathing. By comparing sequence detection in our real data with that in the same data when randomized (using either of two procedures, one preserving the interval structure of each spike train, and so the more conservative), we find that the incidence of sequences is very much greater in the real than in the random data. Further, in cases where recordings were terminated before completion of the full recording session, the difference between pattern detection in real data and that of randomized data strongly correlated with the physiological condition of the animal—in recordings leading to the preparation becoming physiologically unstable, the number of patterns detected in real data approached that in the randomized data. We conclude that such sequences are an important physiological property of the neural system studied, and suggest that they may form a basis for encoding sensory information.

Key words T-pattern analysis, Spike patterns, Neuronal network, Olfactory bulb, Rat

1 Introduction

Much of the computational power of the brain undoubtedly resides in the activities of cooperating and competing networks of neurons. Functional coupling between simultaneously sampled neurons in an in vivo preparation was first reported 1963 by Griffith and Horn [1] and has long been recognized as theoretically important in neuroscience. Synchronized activation between neurons has been linked to perceptual cognition, namely "the binding problem" [2], whereby the combined features of a complex

stimulus are associated by the synchronization of the activities of neurons responding to one or more of those features. The most widely accepted theory of the physiology of memory formation [3], is also based upon the occurrence of such interactions in memory systems—"When an axon of cell A is near enough to excite B and repeatedly or persistently takes part in firing it… A's efficiency, as one of the cells firing B, is increased."

Experimental models have provided evidence that memory formation may adhere to so-called "Hebbian" principles. Long-term potentiation (LTP) is a physiological process that has been studied extensively since its first description in 1974 by Bliss and Lomo [4]. In LTP, presynaptic and postsynaptic elements in a neural pathway are simultaneously activated by repeated electrical stimulation of the presynaptic elements, thereby fulfilling the first of Hebb's principles [3]—neuron A repeatedly activates neuron B through the synaptic connection between the two elements. Subsequently, the efficiency of neuron A in activating neuron B is increased, and so a simple hebbian assembly is formed. In this paradigm, a large number of *neuron A's* activate a large number of *neuron B's* (i.e., there is little noise in the system), and the enhanced efficiency of transmission from one to the other is evident in the increased amplitude of the field potential generated when a single pulse is delivered to the presynaptic elements. However, evidence for such a process occurring across a single synapse in a functioning system remains elusive.

Attempts have been made to discover spike patterns within populations of neurons, but so far these have not produced the desired kinds of results. Thus, Abeles [5] proposed a search algorithm for the detection of multi-neuron patterns called "synfire." While numerous patterns were detected, doubt remains regarding the statistical significance of the findings [6, 7]. In this chapter, a more flexible pattern model, called a T-pattern, is applied (see Chapter 1 in this volume). T-pattern detection uses an evolution algorithm for the detection of the repeated hierarchical and multi-ordinal real-time patterns in data sets consisting of a number of time point series all occurring within the same observation period [8–10]. The large number of T-patterns detected frequently far exceeds those found in randomized data thus the complex patterns discovered through T-pattern analysis provide a dynamic view of neuronal interaction which may be invaluable in understanding the mechanisms of neuronal networks and the way they encode sensory information.

Olfactory encoding is of specific interest as behavioral paradigms underpinning studies of the neurobiology of olfactory learning and memory are considered particularly robust [11] and considerable progress has been made in establishing the neural substrates and pathways involved [12–14]. Much of the encoding takes place at the level of the olfactory bulb (OB), the primary cortical projection area for olfactory input, and an area that is

entirely committed to processing this information. Structurally, the OB is widely conserved across vertebrate taxa. The area has been confirmed as playing an important role in olfactory memory formation. Thus, understanding the processes involved in encoding olfactory information is of great importance to understanding the fundamental neuronal mechanisms of learning and memory. Olfactory receptor neurons in the olfactory epithelium in the nasal cavity project mitral cells in glomeruli in the OB [15]. Optical imaging studies demonstrate that different odorants elicit spatially defined spatial patterns of glomerular activity in the olfactory bulb [16, 17]. The quality of an olfactory stimulus is thus encoded by the combined specific activation of glomeruli by a given odorant. Gaining access to the olfactory bulb with a microelectrode array (MEA) allows in vivo electrophysiological sampling of neuronal activity over a relatively large area of cortex (>2 mm^2). We have applied t-pattern analysis to spike data collected simultaneously across many OB neurons, using microelectrode arrays [18], and established that recurring complex sequences of spikes can be detected in the activity sampled across the mitral cell layer of the OB. These patterns have been characterized in light of a putative role in processing sensory information.

2   Methods

The present data were collected from the olfactory bulb of anesthetized rats (see Fig. 1 for further details). Throughout surgical and experimental procedures, humidified air was supplied through a mask over the nose, and breathing was monitored and recorded using a thermistor in the mask. Data were sampled in 10s periods (trials) at 5 min intervals through a recording session of 6 h, or for as long as the animal remained physiologically stable as judged by its breathing. Some animals reached a point when irregular breathing clearly indicated degrading physiological condition. In such cases recordings were terminated, and degrading condition noted as an experimental variable. Here we compare one such animal with another which remained physiologically viable throughout the full sampling period.

Microelectrode arrays of sharpened tungsten electrodes, arranged in a 6 × 5 array with 350 μ spacing, were advanced laterally into the OB (for one animal a 6 × 8 electrode array, with 250 μ spacing was used). Action potentials (spikes) were sampled from mitral layer OB neurons across an area of ~2.2 mm^2 using a 100 channel laboratory interface (Bionic Technologies Inc./ Cyberkinetics Inc., USA). Spikes sampled in the mitral cell layer are assumed to be generated by mitral cells, as the other cell type in this layer, the granule cell, does not possess an axon [19]. After completion of recordings, offline discrimination of spikes from
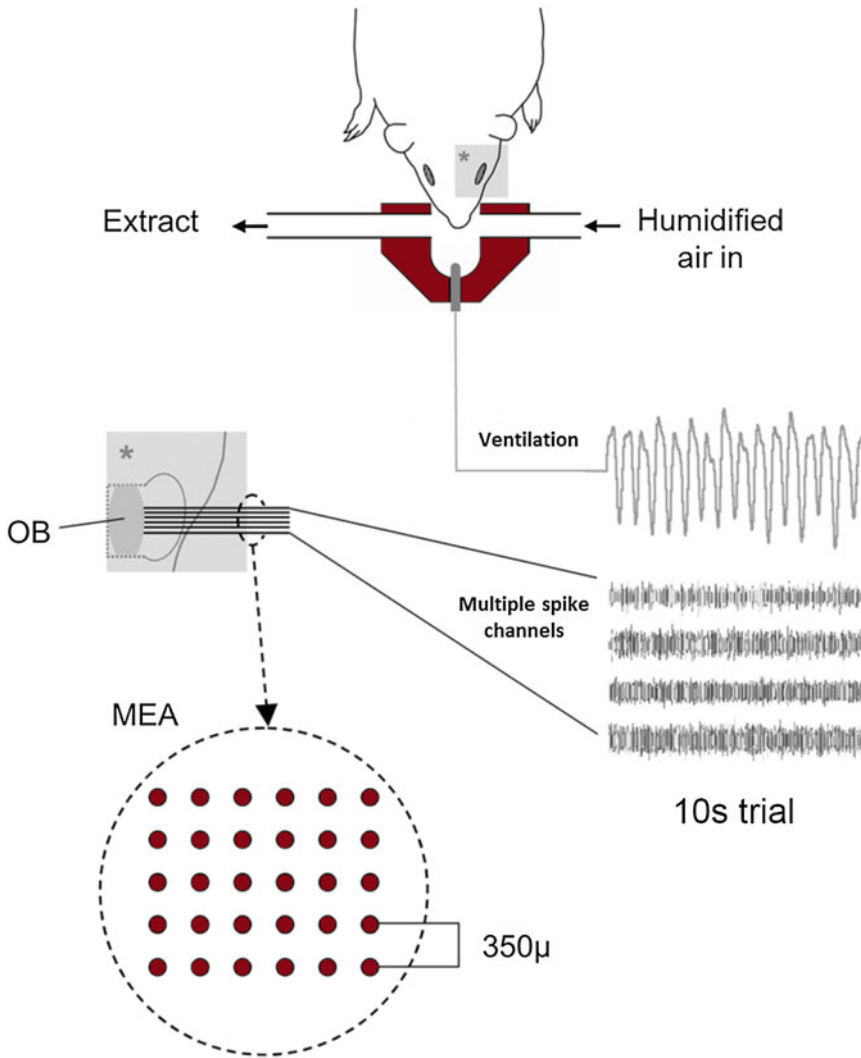
Fig. 1 Action potentials (spikes) from individual neurons were sampled from the olfactory bulb of urethane-anesthetized rats using a microelectrode array positioned laterally in the mitral cell layer of the olfactory bulb of urethane-anesthetized rats. Each electrode in the array could sample spikes from multiple neurons. Here, individual neurons are coded in varied greyscale in the four traces displayed. Humidified air was supplied through a mask over the nose, and breathing was monitored and recorded via a thermistor in the mask

individual neurons was performed using a spike sorting procedure based upon machine learning algorithms to combine the features acquired using principle components analysis (PCA) with features describing the geometric shapes (curvature) within the spike waveform. This procedure was developed specifically to process these data and allows discrimination of activity from multiple neurons at each active electrode [20]. Typically, spikes were sampled simultaneously from ≥100 neurons across the array. Times of occurrence of spikes generated by individual neurons were stored as events coded with the identity of the neuron and its location on the
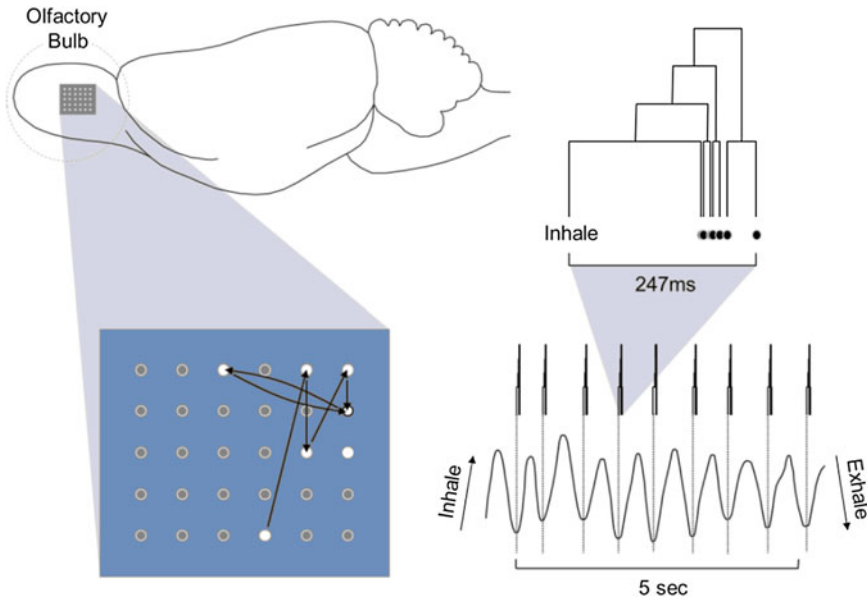
Fig. 2 An example breathing-related sequence of spikes across the olfactory bulb. This pattern spanned the full vertical extent of the 6×5 microelectrode array, incorporating 6 neurons, each sampled on a separate electrode in the array. One neuron, sampled at the electrode (*outlined in black* on the array), was activated twice in the sequence, and provided the final spike in the pattern. The first event in the t-pattern, not shown on the array, was the onset of inhalation—the sequence of spikes occurred regularly as the animal breathed in

MEA. Also stored were events marking onset of expiration and onset of inspiration in the breathing cycle to allow this data to be related to patterns identified in the neural data. The data stored in this way are suitable for t-pattern analysis using Theme™ software (PatternVision, www.patternvision.com, Iceland). In each trial, data were collected during five consecutive complete breathing cycles, each cycle beginning with the onset of inhalation, and ending with the offset of exhalation (see Fig. 2). Event types entered into t-pattern analyses were times of occurrence of spikes from individual neurons, and times of onset of inhalation and exhalation in the breathing cycle.

3   Results

In these data, the relationship between pattern lengths and firing rates amongst the neurons was not simply determined by a stochastic process. It might be assumed that neurons with higher firing rates would by chance have a greater opportunity to participate in longer patterns. We categorized the neurons as slow, medium, or fast, according to firing rate, based approximately around modal firing rates determined across the entire sample. Slow neurons were sufficiently slow that they contributed to no patterns of any length. Amongst the fast neurons, the *longest* patterns to which these
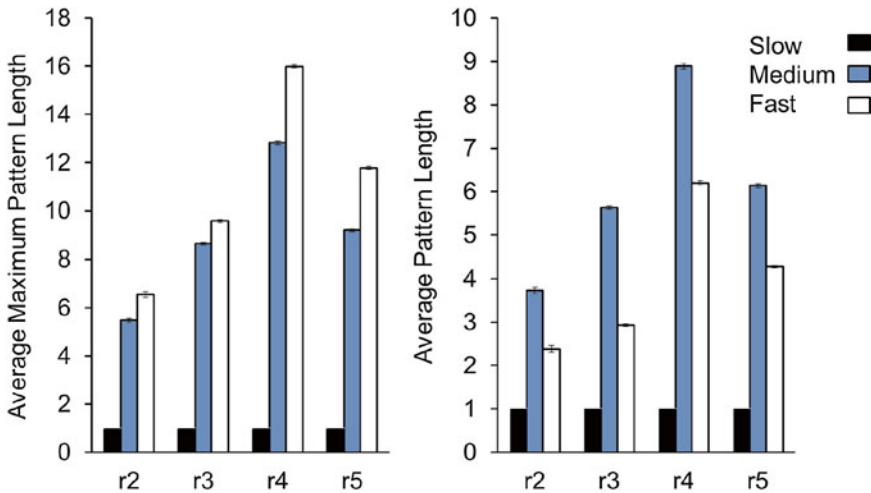
Fig. 3 Distribution of pattern lengths according to neuron firing rate. Neurons were categorized as slow (0–7 spikes), medium (8–100 spikes), or fast (>100 spikes) according the total number of spikes per trial. These firing rates were determined from approximate modal firing rates across the full data set. Slow neurons did not contribute to patterns, and so occur only independently (i.e., pattern length = 1). The remaining fast and medium neurons each, on average, participated in multiple patterns. The average maximum length of pattern that neurons participated in, increased with increasing firing rate. Thus, the average maximum pattern length was longer for fast neurons than for medium neurons. However, this distribution was reversed when considering the average length of patterns in which these neurons participated; the average length of patterns for fast neurons was shorter than that for medium neurons

neurons contributed were indeed longer than those amongst the medium neurons (Fig. 3a). However, conversely to what might have been expected by chance, the *average* length of patterns to which the medium neurons contributed was longer than that for the fast neurons (Fig. 3b). In this way, pattern length is not a simple function of the firing rate of the underlying neurons.

### 3.1 Statistical Validation of T-Patterns

The detection of critical intervals is based on a null hypothesis that is tested a large number of times when seeking patterns in a single data set. Accordingly, many significant patterns are expected to be found even in random data. A crucial issue, therefore, is whether significantly more t-patterns are detected in the initial data than in the same data after they have been randomized. For this the Theme™ software allows randomizing and reanalyzing the data an optional number of times using the same detection parameters as for the real data and then comparing the findings. For this two types of randomization are provided: shuffling and rotation. In both cases the number of series and the number of points in each, remain unchanged.

– *Randomization by shuffling:* Here the time points in each series in the real data are randomly redistributed (shuffled) over the observation period.

– *Randomization by rotation:* This can be imagined thus: all the series in the data set are wrapped around the same cylinder, each series thus forming a circle that is independently rotated by a random number of degrees (0–360°). This procedure, the more conservative of the two, leaves the structure of each series practically unchanged while randomizing the temporal relationship between the series.

By repeatedly randomizing and then searching for patterns in the same data set with the same search parameters as for the real data, an occurrence distribution with mean and a standard deviation is obtained for each pattern length. This allows statistical comparison of the number of patterns of each length detected in the real data as compared to the randomized data and differences can be expressed in terms of the number of standard deviations between the two.

Comparing the lengths and incidence of t-patterns extracted from this data, t-patterns were similarly extracted from the same data when randomized either by shuffling or by rotation. Using either procedure, significantly fewer sequences were detected in the randomized data than in the original electrophysiological data (e.g., see Figs. 4, 5, 6, 7, 8, and 9). The incidence of t-patterns in
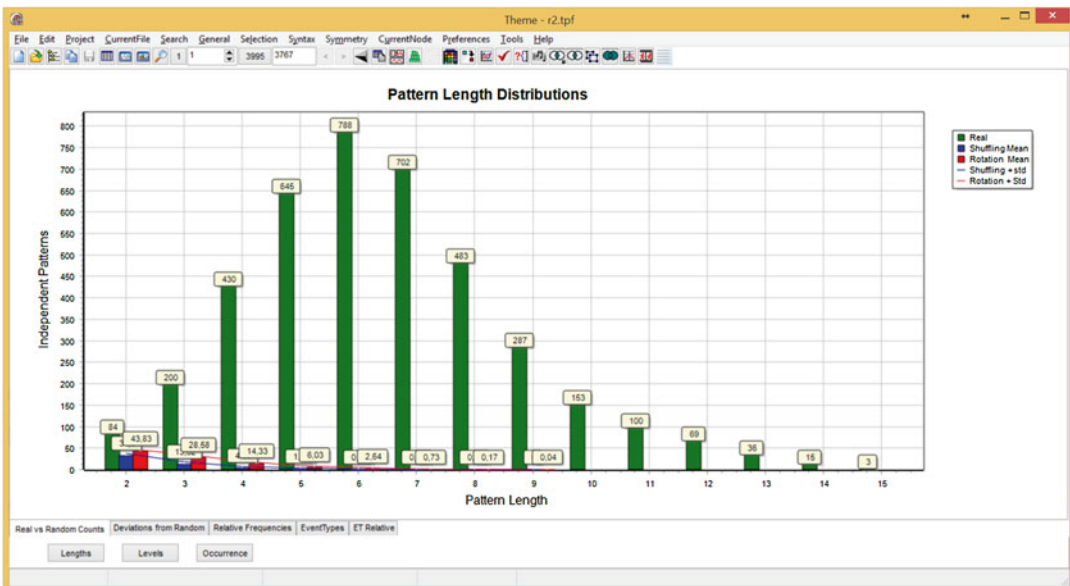
Fig. 4 This chart shows the numbers of different patterns of each length detected in first of the 12 control trials of animal r2, which became physiologically instable and finally had to be terminated after the 12th trial. It also shows the number of different patterns of each length detected on average over 100 repetitions of randomization and search for each of two types of randomization, shuffling and rotation. Here the number of patterns detected and the differences between the real data and the randomized data are at a maximum for the 12 control trials
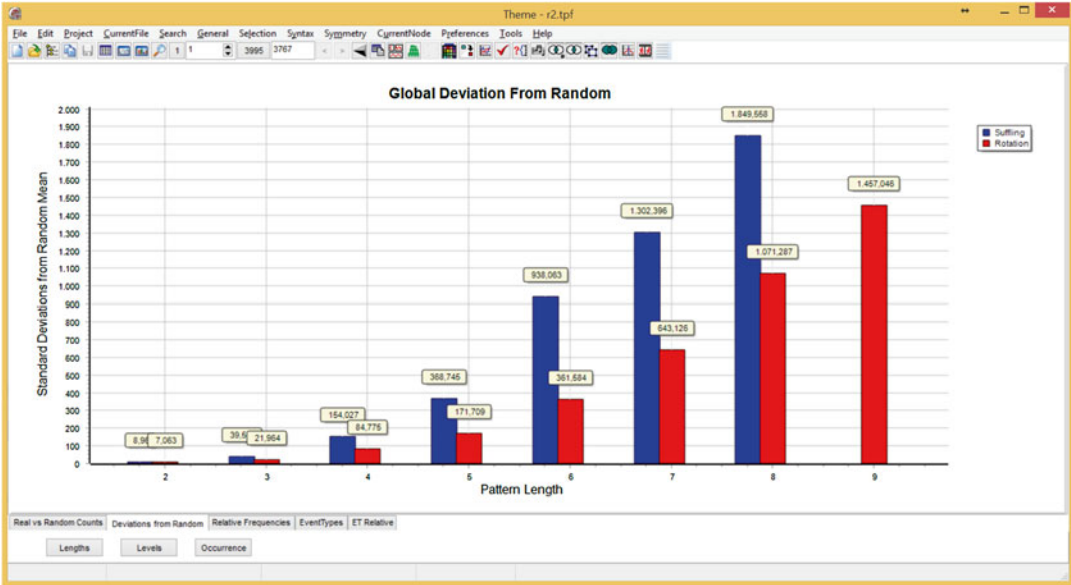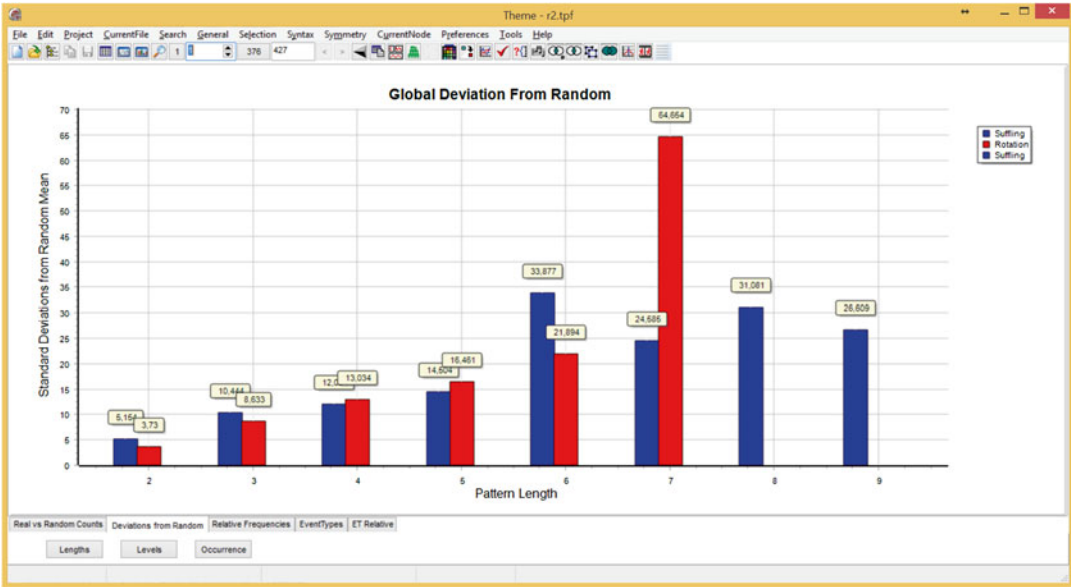
Fig. 5 For the first of the 12 control trials for animal r2 that became instable and finally had to be terminated after the 12th control trial, this chart shows the standardized differences between the numbers of patterns of each length detected in the original data versus the average over 100 repetitions of data randomization and search using the same search parameters. Here these differences are at the maximum for the 12 control trials
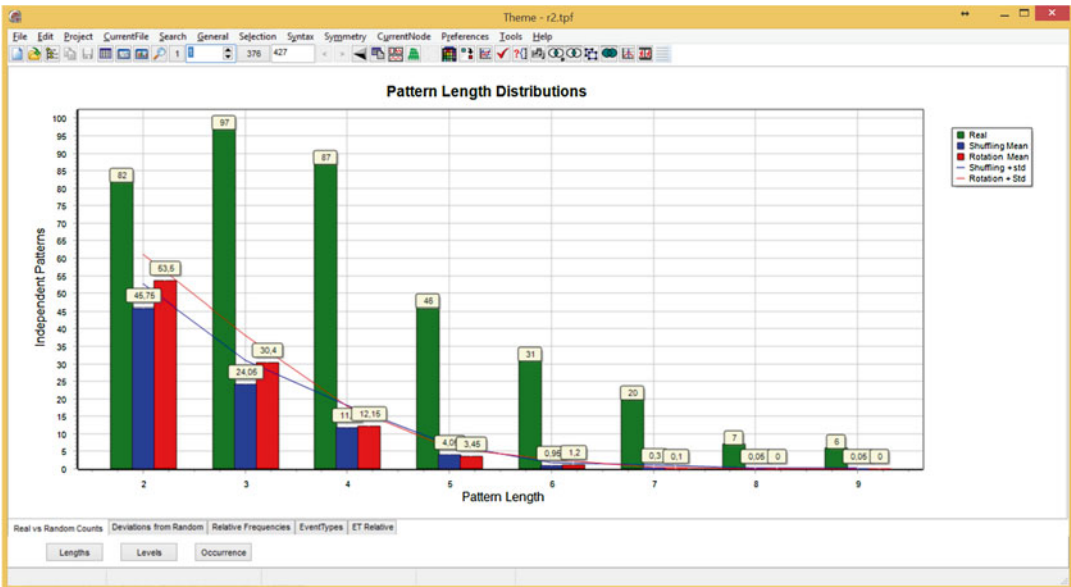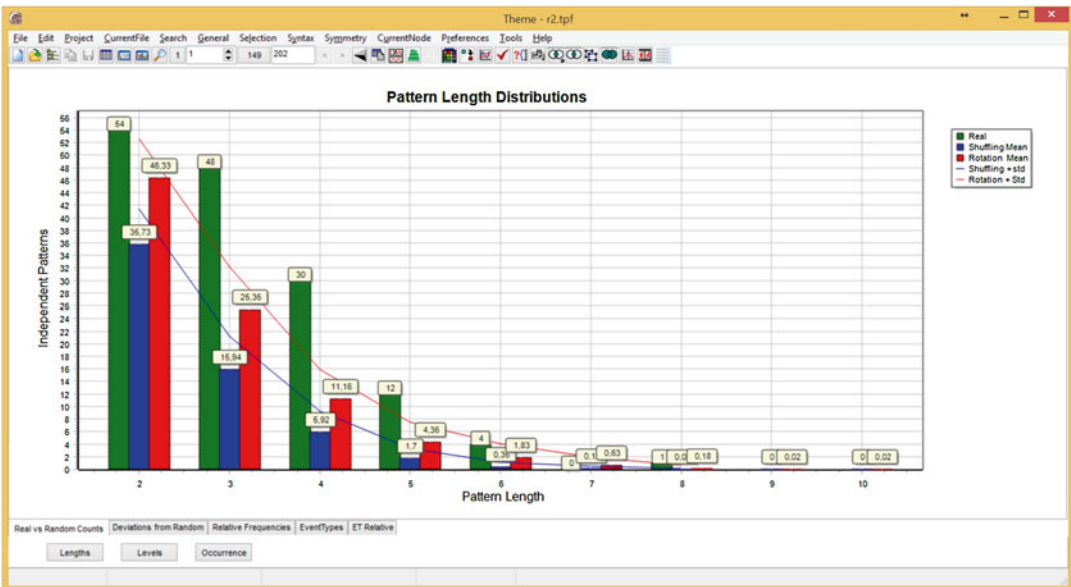

Fig. 6 This chart shows the numbers of different patterns of each length detected in the 7th of the 12 control trials of animal (r2) that became physiologically instable and finally had to be terminated after the 12th trial. It also shows the number of different patterns of each length detected on average over 100 repetitions of randomization and search for two types of randomization, shuffling and rotation. Here the number of patterns detected and the differences of detection between the real data and the randomized data are intermediate between the first and last of the 12 control trials and illustrates the gradual degradation of patterning over the 12 trials
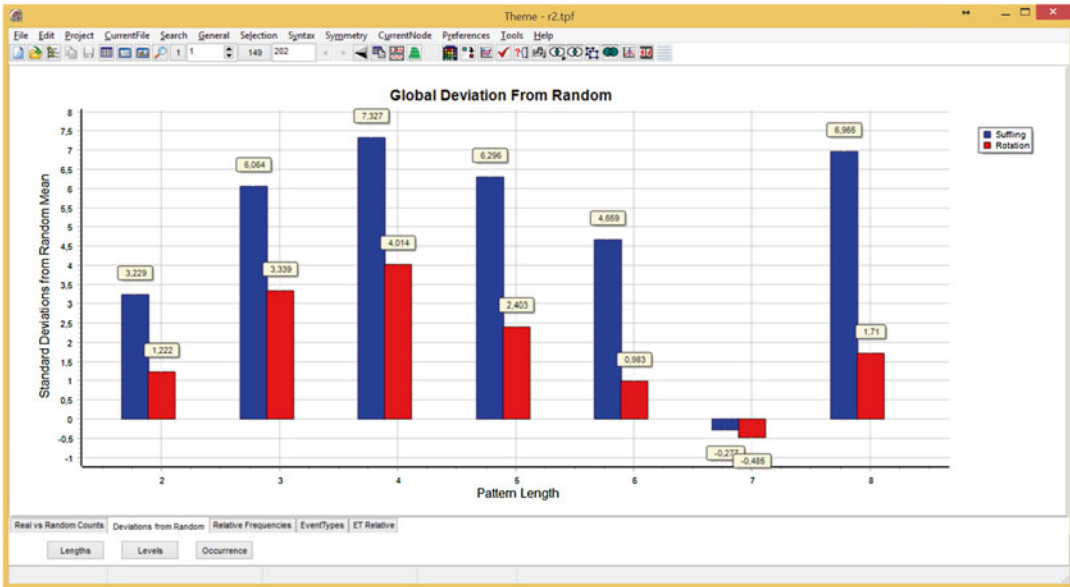
Fig. 7 For the 7th of the 12 control trials for animal (r2) which became instable and finally had to be terminated after the 12th trial, this chart shows the standardized differences between the numbers of patterns of each length detected in the original data versus the average numbers over 100 repetitions of data randomization and search with the same search parameters. Here these differences are at an intermediate level for the 12 control trials

Fig. 8 This chart shows the numbers of different patterns of each length detected in the last of the 12 control trials of an animal (r2) that became physiologically instable and finally had to be terminated after this trial. It also shows the number of different patterns of each length detected on average over 100 repetitions of randomization and search for each of two types of randomization, shuffling and rotation. Here the number of patterns detected and the differences of detection between the real data and the randomized data are at the minimum for the 12 control trials

Fig. 9 For the last of the 12 control trials for an animal (r2), which became instable and finally had to be terminated after this 12th and last trial, this chart shows the standardized differences between the numbers of patterns of each length detected in the original data versus the average over 100 repetitions of data randomization and search with the same search parameters. Here these differences are at the minimum for the 12 control trials

the real data was far greater compared to either type of randomized data. Moreover, the differences were generally much greater for the longer (and a priori less probable) patterns. The number of patterns under randomization as a percentage of patterns in real data also fell rapidly with pattern length dropping to just a few percent or less for the longest patterns.

Although the difference between real and randomized data was often smaller when the more conservative rotation method was used to randomize the data, this difference was nonetheless highly significant. The number of patterns of the same length (m) detected in the original data was thus 5–1000 standard deviations greater than the mean number of patterns in the randomized data, increasing with pattern length, corresponding to significance levels far lower than 0.0001.

In the case of the subject for which recordings were terminated early when irregular breathing indicated deteriorating physiological condition, the difference between T-pattern incidence in random data and that in real data decreased through the recording session. This decrease in the distinction between random and real data continued until the termination of recordings. At that point, there was relatively little difference between t-pattern incidence in real data and that in either form of randomized data (see Fig. 10), although
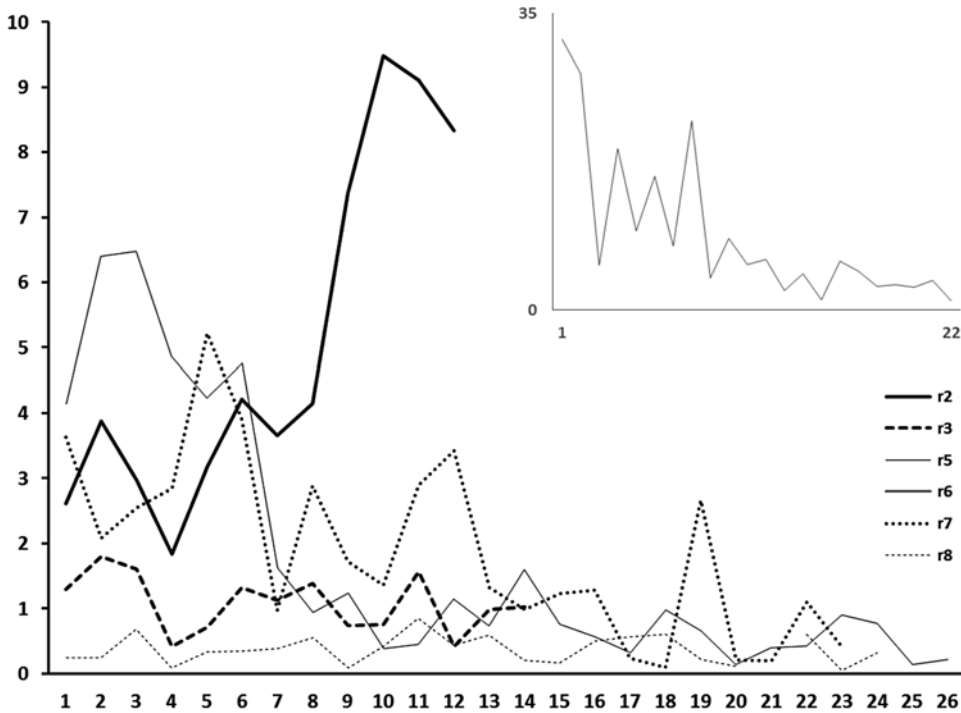
Fig. 10 Relative incidence of patterns in real and randomized data. The average incidence of patterns of any length in 20 randomizations of the data was compared to the pattern incidence in the real data. Here, pattern incidence in randomized data is expressed as a percentage of that in the real data. Data were randomized using the conservative rotation procedure described in the text. In the data from all but one of the animals, the difference in pattern detection between real and randomized data was large throughout the series of recordings, tending to increase as the recordings progressed, i.e., the ratio of patterns in randomized data to those in the real data declined across trials. However, in subject r2, the relative separation in pattern incidence between randomized and real data, whilst maintaining a level similar to that in other animals through the initial 5–6 trials, subsequently degraded (see also Figs. 4, 5, 6, 7, 8, and 9). This accompanied a deterioration in the physiological condition of the anesthetized animal, to the point when recordings were stopped. In another subject animal, r6 (*inset*), separation between randomized data and real data in the early trials was relatively poor, but improved through the series. For this animal, less time was allowed for the animal to stabilize after initial anesthesia and surgical preparation before commencing recordings. It may be that, in this case, consistent with r2, the relative incidence of patterns in randomized and real data reflects the stability of the preparation

the combined firing rates of the neurons remained relatively unchanged, and were even slightly increased, that is, from total of 3042 spikes over all 39 neurons in the first trial to 3114 over all 43 neurons in the last.

3.2 Breathing and Neuronal Firing Patterns

As would be expected, independently of neuronal firing, the breathing cycle was detected in all data sets as two-element (length = 2) t-patterns relating only the two different markers of ventilation (i.e., onset of inhalation and onset of exhalation)

which regularly alternate. Numerous relationships were detected between the breathing markers and (a) the firing of individual neurons and (b) multi-neuron t-patterns. Thus approximately 3–5 % of the t-patterns detected in all data sets analyzed were related to breathing as they included either one or both of the markers of ventilation (e.g., see Fig. 2) and all ventilation events were involved in at least one neuronal firing t-pattern. When only the breathing event series were randomized in the original data and a pattern search performed using the same search parameters as before, no patterns relating breathing and spikes were detected. This was consistent over all files and subjects indicating a highly significant synchronization between breathing and neuronal activity. Figures 11 and 12 show two examples of the kind of T-patterns detected, but these were chosen as they are among the relatively few where each T-pattern occurrence covers a full breathing cycle and, moreover, contain bursts (T-bursts) in one or more neurons. (Regarding T-bursts and T-pattern diagrams see Chap. 1 in this volume.)
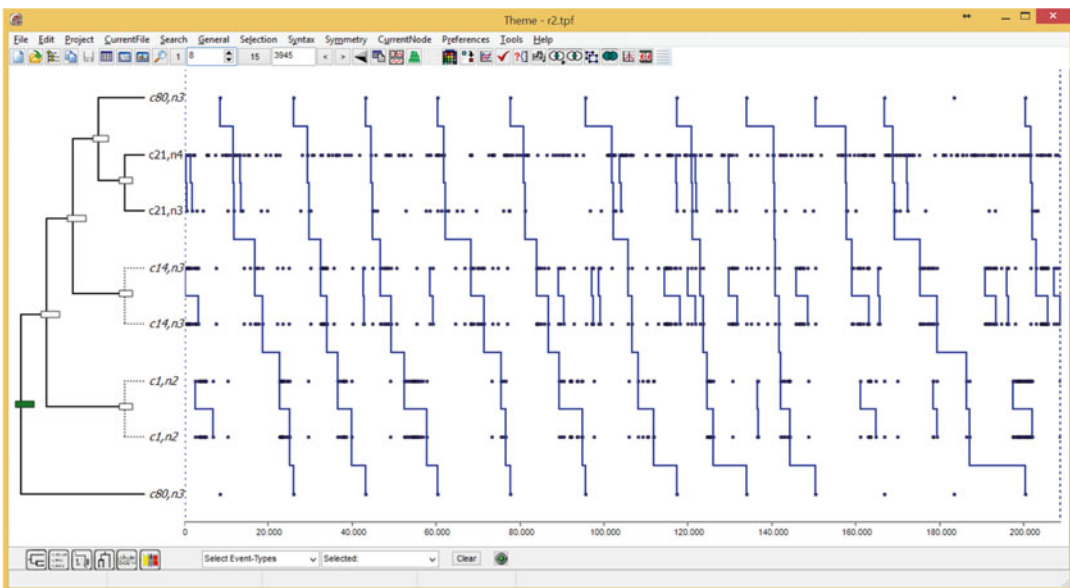
Fig. 11 This T-pattern diagram shows one pattern detected in the first of the 12 control trials for an animal (r2) that later became instable and finally had to be terminated after the 12th trial. The pattern shown is one of the 15 different patterns and with occurrences spanning a full breathing cycle, that is, from one exhale event (c80, n3) to the next, and containing bursts (T-bursts) in individual neurons. Note that this pattern includes a kind of cascade of bursts, that is, first in neuron c14, n3 and then in neuron c1, n2. About T-bursts and T-pattern diagrams see Chapter 1 in this volume (Magnusson)
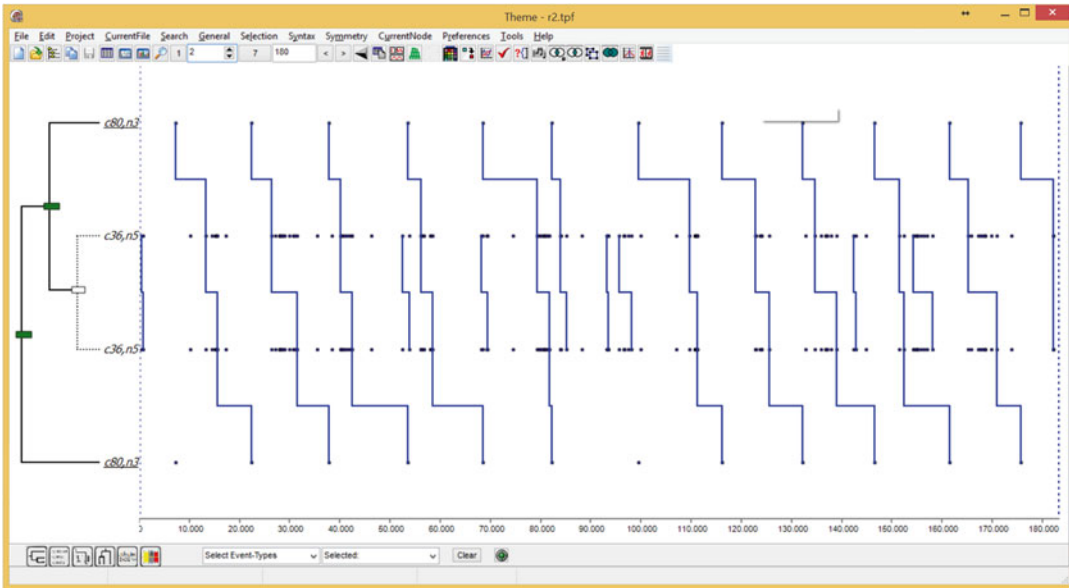
Fig. 12 This T-pattern diagram shows one pattern detected in the last of the 12 control trials in animal (r2) that had become instable and had to be terminated after this 12th control trial. At this point, all patterning had become minimal compared to the initial trial. The figure shows the only pattern containing a burst (T-burst) in one neuron with occurrences spanning a full breathing cycle, that is, from one exhale event (c80, n3) to the next. The burst connecting the two exhale events is in neuron c36, n5. About T-bursts and T-pattern diagrams see Chap. 1 in this volume (Magnusson)

4   Discussion

In the present work we show that complex sequences occur across large areas of the two-dimensional network of mitral neurons in the olfactory bulb. The occurrence of all lengths of these patterns is many times greater than that would be expected by chance. The patterns detected incorporated functional connections spanning in some cases the entire area sampled by the MEA (>2 mm^2). This is perhaps less remarkable given the presence of anatomical connections (paradoxically termed "short axons") spanning many (≤ 30) mitral cells across the olfactory bulb [21].

Precisely timed sequences have previously been described for neuronal firing in cortical neurons [5] and in simulated neuronal networks [22, 23]. Such "synfire" sequences in spontaneous cortical neuronal activity have been reported in intracellularly recorded postsynaptic potentials and in extracellularly recorded spikes both in an isolated tissue preparation and in vivo [24]. Synfire patterns are in some ways similar to t-patterns and may be simply described as t-patterns where all critical intervals are of the same very short length (one millisecond?), that is, $[d_1 + 1]$. However, critics of the synfire algorithm have noted that the incidence of sequences extracted from electrophysiological data using this procedure, may

differ little (nonsignificantly) from the incidence of those similarly extracted from random data [6, 7]. Thus it may be that synfire sequences are largely artifactual, reflecting the particular structure of the underlying series rather than dependencies between those series (cf 25). In this respect t-patterns differ markedly from synfire patterns as the number of t-patterns detected in our electrophysiological data greatly exceeds that detected in randomized data, irrespective of the method employed for randomization (from 5 to 1000 standard deviations, depending respectively on whether randomization is effected using the conservative rotation procedure or by shuffling, as described in this paper).

The algorithm used in t-pattern analysis differs profoundly from the synfire algorithm. In t-patterns, the spikes of neurons A and B (or patterns of such) are connected if, more often than expected by chance, they occur in sequence such that after A there is at least one occurrence of B within particular time window (interval), and the critical interval is neither user defined nor uniquely fixed, but each critical interval relationship is detected by a special algorithm. The synfire detection algorithm does not search for critical interval relationships between events, but attempts to match the spike data to a user-defined interval that typically is very short, conforming to acknowledged synaptic physiological properties, i.e., synaptic delay in the order of a few milliseconds. The interval is thus also constant from one pair of neurons (and/or neuronal patterns) to another, whereas the intervals in t-patterns are variable and automatically detected as a function of the actual data.

The constraints imposed on the biological system in relying on a precise, inflexible, and short interval to establish sequences across multiple neurons, may be, and indeed might be expected to be, extreme. In a neuronal system, a postsynaptic neuron may receive many inputs from many afferent neurons. Some of those inputs are excitatory, others inhibitory. The activation of the postsynaptic neuron is dependent on the summative influences of those excitatory and inhibitory inputs. Moreover, the synapses themselves are subject to failure [26]. Thus, the activity of a single afferent neuron, whilst having a probabilistic influence over the susceptibility of the postsynaptic neuron to discharge, may have negligible impact on the activity of the postsynaptic neuron relative to ongoing activation by the large number of other presynaptic neurons. The statistical nature of the critical intervals used in t-pattern analysis makes this an ideal technique for the detection of sequences amongst such neuronal populations.

These analyses of spike data recorded simultaneously from multiple olfactory bulb neurons demonstrate the occurrence of repeating patterns of activity, many simple, involving perhaps two or three neurons, but many much more complex, across as many as 20 or more neurons. The incidence of these patterns in our neuronal data was very much greater than in the same data when either of two

randomization procedures was used—often the separation of real and randomized data was in the order of hundreds of standard deviations, implying that these sequences are by no means a chance phenomenon. This was maintained across the series of recordings for all subject animals, with the exception of one, which for unknown reasons became physiologically unstable under anesthesia, and ultimately died before completion of the series of recordings. In the trials leading up to the point at which recordings were terminated, the separation between real and randomized data degenerated progressively until the incidence of patterns no longer distinguished them convincingly, despite there being no corresponding degradation in the combined firing rates of the underlying neurons. Again, this points to the incidence of organized spike sequences being a property of the functioning neuronal system.

Individual neurons sampled from each subject animal varied widely in their firing rates. We considered the possibility that faster neurons might have greater opportunity, by chance, to contribute to longer patterns. However, conversely to what might have been expected by chance, whilst the longest patterns involving fast neurons were longer than those involving medium firing rate neurons, the average pattern length to which faster neurons contributed was in fact shorter than for the medium neurons. This again counters the possibility that chance factors might play a part in the incidence of neuronal sequences detected by t-pattern analysis, and also suggests a dissociation in function between fast and medium neurons.

In addressing the potential physiological function of neuronal sequences in the olfactory bulb, we considered the relationship between sequences and breathing. A sizeable subset of patterns detected incorporated the onset of one or other phase in the breathing cycle, inhalation or exhalation. Thus, these patterns are timed to the animal's ventilation, and are consistent with other observations of neuronal activation in phase with breathing using in vivo optical imaging techniques [17] or electrophysiological techniques [27]. The latter study demonstrated that mitral cell membrane potential fluctuations, and therefore likelihood of discharge, occur in phase with ventilatory rhythm. Here we demonstrate that neuronal activity further involves complex sequences of discharge that are related to ventilatory activity.

These investigations demonstrate that complex sequences of spikes can be detected in a neuronal network using t-pattern analysis. Their incidence is very much greater than can be explained by chance, and this property alone can reflect the physiological condition of the animal. These patterns can be categorized according to discrete physiological functions, and hence may represent an important mechanism for coding odor information in the olfactory bulb. In our ongoing investigations we intend to expand our analyses to establish the utility of complex spike sequences detected by t-pattern analysis in the coding of sensory information in the central nervous system.

References

1. Griffith JS, Horn G (1963) Functional coupling between cells in the visual cortex of the unrestrained cat. Nature 199:893–895

2. Engel AK, Roelfsema PR, Fries P, Brecht M, Singer W (1997) Binding and response selection in the temporal domain—a new paradigm for neurobiological research. Theory Biosci 116:241–266

3. Hebb DO (1949) The organisation of behaviour. Wiley, New York, NY

4. Bliss TVP, Lomo T (1973) Long-lasting potentiation of synaptic transmission in dentate area of anesthetized rabbit following stimulation of Perforant path. J Physiol 232:331–356

5. Abeles M, Gerstein GL (1988) Detecting spatiotemporal firing patterns among simultaneously recorded single neurons. J Neurophysiol 60:909–924

6. Oram MW, Hatsopoulos NG, Richmond BJ, Donoghue JP (2001) Excess synchrony in motor cortical neurons provides redundant direction information with that from coarse temporal measures. J Neurophysiol 86:1700–1716

7. Baker S, Lemon RN (2000) Precise spatiotemporal repeating patterns in monkey primary and supplementary motor areas occur at chance level. J Neurophysiol 84:1770–1780

8. Magnusson MS (2000) Discovering hidden time patterns in behavior: T-patterns and their detection. Behav Res Methods Instrum Comput 32:93–110

9. Magnusson MS (2004) Repeated patterns in behavior and other biological phenomena. In: Kimbrough Oller D, Griebel U (eds) Evolution of communication systems: a comparative approach (Vienna series in theoretical biology). The MIT Press, Cambridge, MA

10. Magnusson MS, Burfield I, Loijens L, Grieco F, Jonsson GK, Spink A (2004) Theme: Powerful Tool for Detection and Analysis of Hidden Patterns in Behavior. Reference Manual, Version 5.0. Noldus Information Technology BV, Wageningen, The Netherlands.

11. Bolhuis JJ, MacPhail EM (2001) A critique of the neuroecology of learning & memory. Trends Cogn Sci 5:426–433

12. Kendrick KM, Levy F, Keverne EB (1992) Changes in the sensory processing of olfactory signals induced by birth in sheep. Science 256:883–886

13. Kendrick KM, Guevara-Guzman R, Zorrilla J, Hinton MR, Broad KD, Mimmack M, Ohkura S (1997) Formation of olfactory memories mediated by nitric oxide. Nature 388:670–674

14. Da Costa APC, Broad KD, Kendrick KM (1997) Olfactory memory and maternal behaviour-induced changes in c-fos and zif/268 mRNA expression in the sheep brain. Mol Brain Res 46:53–76

15. Mori K, Nagau H, Yoshihara Y (1999) The olfactory bulb: coding and processing of odor molecule information. Science 286:711–715

16. Johnson BA, Ho SL, Yihan JS, Yip S, Hingco EE, Leon M (2002) Functional mapping of the rat olfactory bulb using diverse odorants reveals modular responses to functional groups and hydrocarbon structural features. J Comp Neurol 449:180–194

17. Spors H, Grinvald A (2002) Spatio-temporal dynamics of odor representations in the mammalian olfactory bulb. Neuron 34:301–315

18. Nicol AU, Segonds-Pichon A, Magnusson MS (2015) Complex spike patterns in olfactory bulb neuronal networks. J Neurosci Methods 239:11–17

19. Price JL, Powell TPS (1969) The morphology of the granule cells of the olfactory bulb. J Cell Sci 7:91–123

20. Horton PM, Nicol AU, Kendrick KM, Feng JF (2007) Spike sorting based upon machine learning algorithms (SOMA). J Neurosci Methods 160:52–68

21. Aungst JL, Heyward PM, Puche AC, Karnup SV, Hayar A, Szabo G, Shipley MT (2003) Centre-surround inhibition among olfactory bulb glomeruli. Nature 426:623–629

22. Schrader S, Grün S, Diesmann M, Gerstein GL (2008) Detecting synfire chain activity with massively parallel spike train recording. J Neurophysiol 100:2165–2176

23. Gerstein GL, Williams ER, Diesmann M, Grün S, Trengrove C (2012) Detecting synfire chains in parallel spike data. J Neurosci Methods 206:54–64

24. Ikegaya I, Aaron G, Cossart R, Aronov D, Lampl I, Ferster D, Yuste R (2004) Synfire chains and cortical songs: temporal modules of cortical activity. Science 304:559–564

25. Gerstein GL (2004) Searching for significance in spatio-temporal firing patterns. Acta Neurobiol Exp 64:203–207

26. Zador A (1998) Impact of synaptic unreliability on the information transmitted by spiking neurons. J Neurophysiol 79:1219–1229

27. Margrie TW, Schaefer AT (2002) Theta oscillation coupled spike latencies yield computational vigour in a mammalian sensory system. J Physiol 546:363–374